Differences in Left Versus Right Ventricular Electrophysiological Properties in Cardiac Dysfunction and Arrhythmogenesis

Cristina E Molina,[1] Jordi Heijman[2] and Dobromir Dobrev[1]

1. Institute of Pharmacology, West German Heart and Vascular Center, Faculty of Medicine, University Duisburg-Essen, Essen, Germany; 2. Cardiovascular Research Institute Maastricht, Faculty of Health, Medicine, and Life Sciences, Maastricht University, Maastricht, The Netherlands

Abstract

A wide range of ion channels, transporters, signaling pathways and tissue structure at a microscopic and macroscopic scale regulate the electrophysiological activity of the heart. Each region of the heart has optimised these properties based on its specific role during the cardiac cycle, leading to well-established differences in electrophysiology, Ca^{2+} handling and tissue structure between atria and ventricles and between different layers of the ventricular wall. Similarly, the right ventricle (RV) and left ventricle (LV) have different embryological, structural, metabolic and electrophysiological features, but whether interventricular differences promote differential remodeling leading to arrhythmias is not well understood. In this article, we will summarise the available data on intrinsic differences between LV and RV electrophysiology and indicate how these differences affect cardiac function. Furthermore, we will discuss the differential remodeling of both chambers in pathological conditions and its potential impact on arrhythmogenesis.

Keywords

Regional differences, ventricular function, right and left ventricle, cardiac remodeling, ventricular arrhythmias

Disclosure: The authors have no conflicts of interest to declare.

Acknowledgement: The authors' current work is supported by the German Federal Ministry of Education and Research through DZHK (German Center for Cardiovascular Research, to DD).

Received: 13 January 2016 **Accepted:** 24 March 2016 **Citation:** *Arrhythmia & Electrophysiology Review* 2016;**5**(1):14–9 **Access at:** www.AERjournal.com

DOI: 10.15420/AER.2016.8.2

Correspondence: Prof Dr Dobromir Dobrev, Institute of Pharmacology, Hufelandstr 55, D-45122 Essen, Germany. E: dobromir.dobrev@uk-essen.de

Optimal cardiac function depends on appropriate rate and force of contraction, with specific cardiac regions having developed particular beat-to-beat properties depending on their individual functions. For example, isovolumetric contraction time is shorter in the right ventricle (RV) than in the left ventricle (LV). At the cellular level, cardiac function is regulated by regional cardiomyocyte electrophysiological and Ca^{2+}-handling properties (see *Figure 1*). Differences in these properties between nodal cells and working myocardium,[1,2] atrial and ventricular cardiomyocytes[1,3,4] and different layers of the LV wall (endo-, mid- and epicardium)[5–7] have been well established. Although electrophysiological differences between left and right sides of the heart have been less extensively characterised there is evidence for clinically relevant left-to-right differences in the atrium[1,8–10] and the ventricle.[1,5,11–14] Here, we review the known differences in LV and RV electrophysiology and Ca^{2+} handling at baseline and during pathophysiological conditions. Furthermore, we discuss the implications of these differences for arrhythmogenesis.

Basic Cardiac Electrophysiology and Arrhythmia Mechanisms

Cardiac excitation–contraction (EC) coupling is a sequence of events occurring in cardiomyocytes upon electrical activation, resulting in the generation of an action potential (AP) and subsequent cardiomyocyte contraction (see *Figure 2*). This sequence shows many similarities between different cell types, notably between LV and RV cardiomyocytes. In this section we briefly summarise the common features.

EC coupling involves an initial depolarisation of the membrane potential due to activation of Na^+ channels and consequent opening of voltage-dependent K^+ channels and L-type Ca^{2+} channels. The K^+ channels consist of delayed-rectifier channels with distinct kinetics, underlying a transient-outward K^+ current (I_{to}), as well as rapid and slow delayed-rectifier K^+ currents (I_{Kr} and I_{Ks}, respectively). These currents play a major role in the AP repolarisation and critically determine AP duration (APD). The inward-rectifier K^+ current (I_{K1}) activates late during the AP and controls final repolarisation and resting membrane potential stability. L-type Ca^{2+} channels activate early during the AP and provide a depolarising current ($I_{Ca,L}$). Although the current subsequently declines due to voltage- and Ca^{2+}-dependent inactivation, it supports the plateau phase of the ventricular AP (see *Figure 2A*). Moreover, the Ca^{2+} entering the cardiomyocyte through L-type Ca^{2+} channels plays a critical role initiating EC coupling by activating type-2 ryanodine receptor (RyR2) channels on the sarcoplasmic reticulum (SR) membrane, producing a much larger SR Ca^{2+} release. This process is termed Ca^{2+}-induced Ca^{2+} release (CICR) and results in an increase in the cytoplasmic Ca^{2+} concentration sufficient to activate the contractile apparatus, initiating cardiomyocyte contraction.[15] Subsequently, resequestration of Ca^{2+} in the SR by the SR Ca^{2+} ATPase type-2a (SERCA2a) and extrusion of Ca^{2+} to the extracellular space by the Na^+-Ca^{2+} exchanger type-1 (NCX1) returns cytosolic Ca^{2+} to diastolic levels, promoting cellular relaxation. Finally, ionic homeostasis of intracellular Na^+ and K^+ is maintained by the Na^+/

K^+-ATPase and the resulting current (I_{NaK}) contributes to membrane repolarisation and stability of the resting membrane potential.

Cardiac arrhythmias can arise when normal impulse generation or impulse propagation is compromised.[16] Abnormal impulse formation outside of the sinoatrial node (ectopic activity) generally results from instabilities of the membrane potential during or after the AP (termed early or delayed after depolarisations [EADs/DADs]). EADs are promoted by excessive APD prolongation (e.g., due to loss of repolarising K^+ currents), resulting in $I_{Ca,L}$ reactivation and secondary depolarisations.[17] DADs, on the other hand, result from spontaneous SR Ca^{2+}-release events that activate NCX1. Since NCX1 is electrogenic (exchanging one Ca^{2+} for three Na^+), this produces a transient inward current and depolarisation of the membrane potential.[18–20]

When EADs or DADs of sufficient amplitude occur synchronised between a large enough number of cells, the electrical activity can propagate through the remainder of the myocardium as ectopic (triggered) activity. Impulse propagation is mainly determined by electrical cell-to-cell coupling through gap-junction channels, presence of non-conducting tissue (non-excitable cells, fibrosis), and the local source/sink balance (e.g., depending on I_{Na} availability). Slow, heterogeneous conduction and short effective refractory periods promote reentrant activity, the predominant arrhythmia maintaining mechanism.[21,22] Both ectopic activity and reentry are promoted by electrical, structural and neurohumoral ventricular remodeling, occurring in both hereditary and acquired cardiovascular diseases.

Differences Between Left Ventricle and Right Ventricle Cellular Electrophysiology at Baseline and During Pathophysiological Remodeling

Differences in Ion Channel Properties

The AP is generated by specific voltage-gated ion currents so it is logical that electrophysiological differences between heart chambers result in large part from differences in ion currents (see *Figure 3*).[1] Indeed, electrophysiological specialisation of different regions of the heart has resulted in characteristic AP patterns for each region (see *Figure 1*).[6]

Potential ionic differences between basal LV and RV cellular electrophysiology have been identified at the mRNA, protein and functional levels (see *Table 1*). In most species and experimental models, the RV myocardium shows a relative overexpression of $K_v4.2$, $K_v4.3$ and KChIP2,[23,24] molecular components of I_{to}, as well as greater *KCNQ1* expression,[25,26] part of the I_{Ks} macromolecular complex. In agreement, a number of studies observed larger I_{Ks} and I_{to} in RV compared with LV.[27–30] In addition, some studies have observed changes in the gene expression of $K_{ir}6.1/K_{ir}6.2$, underlying the ATP-sensitive K^+ current (I_{KATP}),[31,32] *NCX1*[33] and $K_{ir}2.1/K_{ir}2.3$, molecular components of I_{K1}.[34,35] Consistent with these molecular data, I_{K1} density is larger in LV myocytes from guinea pigs, contributing to the stabilisation of the high-frequency rotors in LV.[36,37] However, other studies in different animal models did not find a significant difference between LV and RV I_{K1}.[28,29] Finally, some studies have suggested that I_{Na} might be smaller in RV than LV.[23,35]

At the cellular level, APs showed deeper notches, shorter APDs at 50 % and 95 % of repolarisation and less APD prolongation on slowing of the pacing rate in RV than LV,[27,24,29] consistent with the larger I_{to} and I_{Ks}. Similarly, duration of monophasic APs *in vivo* was shorter in RV than in LV.[25] Resting membrane potential and AP upstroke velocity did not differ between LV and RV in these studies.[27,29]

Figure 1: Schematic Representation of the Electrophysiological Properties of Different Regions in the Heart

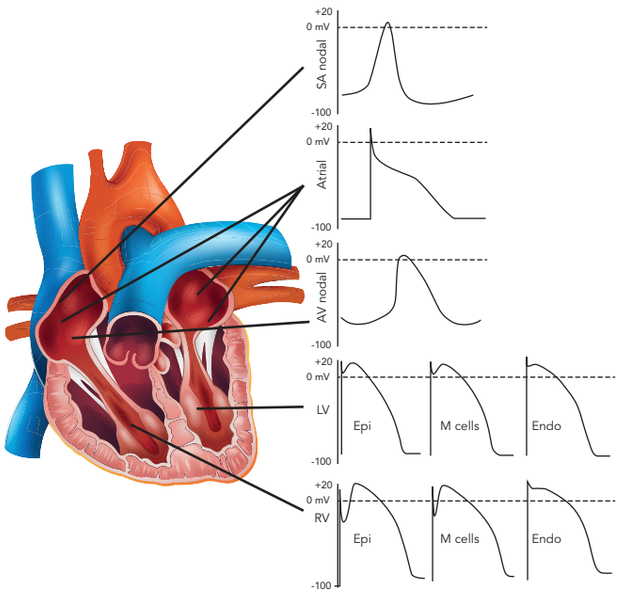

Representative action potential waveforms from different regions of the heart are shown. AV = atrioventricular node; Endo = cardiomyocytes from endocardium; Epi = cardiomyocytes from epicardium; LV = left ventricle; M Cells = cardiomyocytes from midmyocardium; RV = right ventricle; SA = sinoatrial node. Adapted based on experimental traces from Diego et al.,[27] Nerbonne et al.[63] and Volders et al.[64]

Figure 2: Key Ion Currents Shaping the Cardiac Action Potential

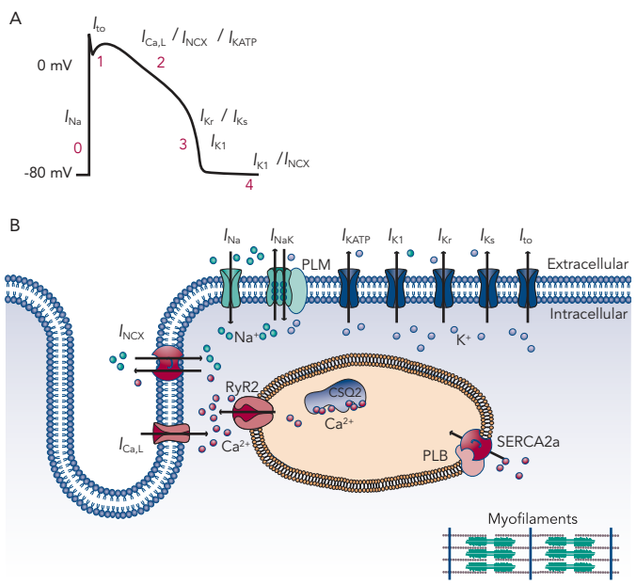

A: Schematic action potential, its phases and the ionic current contribution to the action potential. CSQ2 = calsequestrin 2; PLB = phospholamban; RyR2 = type-2 ryanodine receptor; SERCA2a = sarcoplasmic reticulum Ca^{2+} ATPase type-2a; I_{Na} = Na^+ current; I_{to} = transient outward K^+ current; $I_{Ca,L}$ = L-type Ca^{2+} current; I_{NCX} = Na^+-Ca^{2+} exchange current; $I_{K,ATP}$ = ATP-sensitive K^+ current; I_{Kr} = rapid component of delayed-rectifier K^+ current (I_K); I_{Ks} = slow component of I_K; I_{K1} = inward-rectifier K^+ current. B: Representation of ion currents and Ca^{2+} handling proteins in ventricular cardiomyocytes.

Although these results clearly suggest different electrophysiological phenotypes of the RV and LV, there is significant disagreement between the different species and experimental settings, as well as between expression data and functional studies. I_{to} is a notable exception being consistently larger in RV than LV (see *Table 1*). Furthermore, the role of individual electrophysiological differences in chamber-specific

Figure 3: Representative Right and Left Ventricular Action Potential Waveforms, Chamber-specific Ion Channel Regulation and Statistically Significant Gene Expression Differences

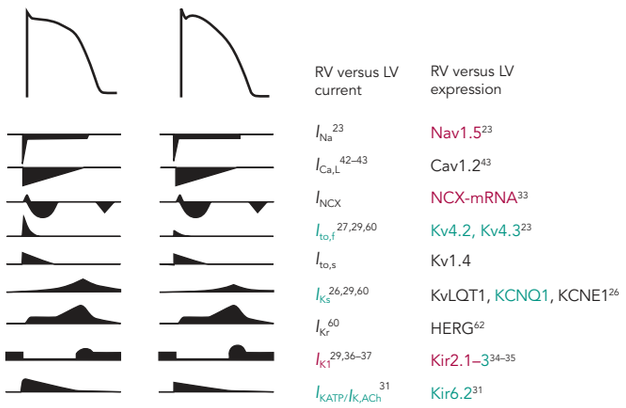

Ionic currents involved in the initiation and maintenance of an action potential (AP) and their chamber-specific differences. Green means up-regulation and red down-regulation in RV versus LV and black indicates no change between chambers. LV = left ventricle; RV = right ventricle. Underlying experimental data are summarised in Table 1.

proarrhythmia is largely unknown. Similarly, only a limited number of studies have investigated whether chamber-specific electrical and structural remodeling processes regulate these differences between both ventricles. Volders et al.[30] reported an RV-specific downregulation of I_{Kr} and a disappearance of the LV/RV differences in I_{Ks} in a dog model with chronic complete atrioventricular block. These findings were confirmed at the transcriptional level by downregulation of *KCNH2* and *KCNQ1* expression (underlying I_{Kr} and I_{Ks}, respectively) in subsequent studies.[24,25] Reduction of repolarisation reserve due to K^+-channel downregulation is linked to an increased risk of ventricular arrhythmias and sudden cardiac death in this experimental model. Differences in I_{to} between LV and RV, on the other hand, remained intact in this model, highlighting the complexity of chamber-selective and channel-specific remodeling.

Differences in Ca^{2+} Handling and Contractility

Interventricular differences in Ca^{2+} handling and contractility have been predominantly investigated in rodents (see *Table 1*). No intrinsic RV/LV differences were found in gene expression of SERCA2a, its inhibitory regulator phospholamban (PLB), RyR2, NCX1 or the pore-forming α subunit of the L-type Ca^{2+} channel.[28] Similarly, SR Ca^{2+} uptake was not different between both ventricles. Nonetheless, systolic [Ca^{2+}] and cell shortening were larger in LV than RV. AP clamp experiments showed that the observed interventricular differences in Ca^{2+} handling were due to differences in AP morphology, with shorter APD in the RV compared with the LV, affecting $I_{Ca,L}$-mediated Ca^{2+} influx.[28] SERCA2a and PLB mRNA levels were also similar in both ventricles in rats,[33] whereas protein expression of both was lower in RV.[26] In accordance, SR Ca^{2+} sequestration was slower in RV compared with LV in normal rat myocardium,[38,26] and Ca^{2+}-transient decay was slower in RV.[26] There were no interventricular differences in diastolic or systolic [Ca^{2+}] but cell shortening was smaller in rat RV cardiomyocytes. Furthermore, both ventricles showed opposite changes in SR Ca^{2+} sequestration upon induced myocardial infarction. While in the LV Ca^{2+} uptake decreased, it increased in RV, affecting the rate of relaxation and contraction. This suggests that failure of the LV promotes differential RV remodeling and potentially proarrhythmic chamber dyssynchrony.[38]

There are important differences in electrophysiology and Ca^{2+} handling between rodents and larger mammals (including humans). Rodents rely heavily on SR Ca^{2+} cycling, with >90 % of the total Ca^{2+} flux during a single beat resulting from SR Ca^{2+} release and subsequent SR Ca^{2+} reuptake. By contrast, in larger mammals there is a much larger role for Ca^{2+} entry via $I_{Ca,L}$ and NCX1-mediated Ca^{2+} extrusion, which account for ~30 % of the total Ca^{2+} flux.[39,40] Thus, extrapolation of the data on LV/RV differences in Ca^{2+} handling from rodents to humans is difficult.

There are few data available about chamber-specific Ca^{2+}-handling properties in large mammals. RyR2 mRNA and protein expression were lower in RV compared with LV in myocardium of control dogs.[41] By contrast, RyR2 gene expression was larger in RV in ventricular samples from cardiomyopathy patients.[34] At the functional level, no differences in basal Ca^{2+}-transient amplitude or sarcomere shortening could be detected between RV and LV in canine cardiomyocytes.[42] Cardiomyocyte shortening and relaxation rate in RV and LV were also similar in cats.[43] Interestingly, interventricular differences in RyR2 expression were eliminated, and total RyR2 expression decreased in dogs with arrhythmogenic right ventricular cardiomyopathy.[41] Similarly, Gupta et al.[44] found reduced SERCA2a activity and protein levels in LV, but not RV, in dogs with chronic heart failure, eliminating interventricular differences. These data suggest that interventricular differences in Ca^{2+} handling are species dependent and can be further regulated by chamber-specific disease-related remodeling.

Interventricular Differences in the Regulation of Cardiomyocyte Electrophysiology and Ca^{2+} Handling

Numerous studies have highlighted the importance of post-translational regulation of ion channels and Ca^{2+}-handling proteins to control cardiac electrophysiology and contractility in response to various neurohumoral conditions.[15,45–47] Activation of β-adrenoceptors with isoprenaline similarly regulates $I_{Ca,L}$ and I_{Ks} in canine LV and RV cardiomyocytes, whereas it increased sarcomere shortening 10-fold versus 25-fold and Ca^{2+}-transient amplitude two-fold versus three-fold in LV versus RV cardiomyocytes, respectively, highlighting clear interventricular differences in the regulation of cardiomyocyte Ca^{2+} handling.[42] These differences were found to be due to a selective isoprenaline-induced increase in cytoplasmic cAMP in RV, resulting from distinct rates of cAMP degradation by type-3 and type-4 phosphodiesterases.[42] By contrast, Ca^{2+}/calmodulin-dependent kinase type-II (CaMKII)-dependent phosphorylation of RyR2, SERCA2a and PLB following application of exogeneous calmodulin/Ca^{2+} was reduced in RV versus LV myocardium of rats,[26] thus suggesting potential interventricular differences in CaMKII signaling.

The RV and LV also showed opposite inotropic responses to α1-adrenergic stimulation,[48] which was at least in part due to heterogeneous effects on LV/RV intracellular Ca^{2+} handling.[49] Finally, β2-adrenoceptors were found highly upregulated in LV, but not RV, in rats with chronic mild stress.[50] Thus, although relatively little is known about interventricular differences in ion channel regulation, presently available data suggest a complex system with chamber-specific remodeling of pre-existing interventricular differences in regulatory signaling pathways, which act upon differences in basal LV versus RV electrophysiology and Ca^{2+} handling.

Mechanisms Underlying Left Ventricle versus Right Ventricle Differences

The electrophysiological differences between the LV and RV can at least partially be attributed to the distinct embryological origin

Table 1: Differences in mRNA and Protein Expression and Channel Function Between Left and Right Ventricle for the Major Ion Currents and Ca^{2+} Handling Proteins Reported in the Literature

	Level	RV vs LV	Species/Model	Reference
$I_{Ca,L}$	mRNA (*CACNA1C*)	↔	WT mouse	43
	mRNA (*CACNB2*)	+66 %	Human myopathic hearts	34
	Current	↔	Feline myocardium	43
		↔	WT mouse	28
		↔	Canine midmyocardium	42
$I_{Ca,T}$	mRNA (*CACNA1G*)	+110 %	Human myopathic hearts	34
I_f	mRNA (*HCN2*)	-68 %	Human myopathic hearts	34
I_{K1}	mRNA (*KCNJ2*)	↔	WT and *SCN5A*$^{+/-}$ mouse	23, 65
		-50 %	Guinea pig	37
	mRNA (*KCNJ4*)	-33 %	Human myopathic hearts	34
		-30 %	Guinea pig	37
	Protein ($K_{ir}2.1$)	↔	WT and *SCN5A*$^{+/-}$ mouse	23
		-10 %	Guinea pig	35
	Current	↔	Canine midmyocardium	29, 30
		↔	Midmyocard. CAVB dogs	30
		↔	WT mouse	28
		-40 %	Guinea pig	37
		-30 %	Guinea pig	36
I_{KATP}	mRNA (*KCNJ8*)	-33 %	Guinea pig	32
	mRNA (*KCNJ11*)	-33 %	Guinea pig	32
I_{Kr}	mRNA (*KCNH2*)	+150 %	Human samples	66
		+75 %	Midmyocard. CAVB dogs	24
	Current	↔	Canine midmyocardium	29
		+50 %#	Canine midmyocardium	30
		↔	Midmyocard. CAVB dogs	30
I_{Ks}	mRNA (*KCNQ1*)	+100 %	Human samples	66
		+250 %	Canine midmyocardium	25
		+80 %	Canine septum	24
		+90 %	Canine myocardium	24
		↔	Midmyocard. CAVB dogs	24, 25
	mRNA (*KCNE1*)	+20 %#	Canine midmyocardium	25
		↔	Midmyocard. CAVB dogs	24, 25
	Protein (KCNE1)	+20 %	Canine midmyocardium	25
		↔	Midmyocard. CAVB dogs	25
	Current	+69 %	Canine midmyocardium	29
		+50 %	Canine midmyocardium	30
		↔	Midmyocard. CAVB dogs	30
		+37 %	Canine midmyocardium	42
I_{Kur}	mRNA (*KCNA5*)	↔	WT and *SCN5A*$^{+/-}$ mouse	23
	Protein ($K_v1.5$)	↔	WT and *SCN5A*$^{+/-}$ mouse	23
I_{Na}	mRNA (*SCN5A*)	+50 %	WT mouse	23
		↔	*SCN5A*$^{+/-}$ mouse	23
		↔	Canine midmyocardium	24
	Protein ($Na_v1.5$)	↔	WT mouse	23
		-25 %	*SCN5A*$^{+/-}$ mouse	23
		-18 %	Guinea pig	35
	Current	↔	WT mouse	23
		-35 %	*SCN5A*$^{+/-}$ mouse	23

	Level	RV vs LV	Species/Model	Reference
I_{NaK}	mRNA (*ATP1A3*)	+15 %	Human myopathic hearts	34
I_{NCX}	mRNA (*SLC8A1*)	-50 %	Control rat myocardium	33
		+50 %	Canine septum	24
		↔	WT mouse	28
I_{to}	mRNA (*KCND2*)	+50 %	WT and *SCN5A*$^{+/-}$ mouse	23
		+70 %	WT mouse	65
	mRNA (*KCND3*)	↔	Canine septum	24
		↔	WT mouse	65
		+20 %	WT mouse	23
		↔	*SCN5A*$^{+/-}$ mouse	23
	mRNA (*KCNA4*)	↔	WT and *SCN5A*$^{+/-}$ mouse	23
	mRNA (*KChIP2*)	+400 %	Canine septum	24
		+175 %	Canine myocardium	24
		↔	WT mouse	65
		+50 %	WT mouse	23
		+10 %	*SCN5A*$^{+/-}$ mouse	23
	Protein ($K_v4.2$)	+85 %	WT and *SCN5A*$^{+/-}$ mouse	23
	Protein ($K_v4.3$)	+50 %	WT and *SCN5A*$^{+/-}$ mouse	23
	Protein ($K_v1.4$)	↔	WT mouse	23
		↔	*SCN5A*$^{+/-}$ mouse	23
	Protein (KChIP2)	+25 %	WT mouse	23
		+50 %	*SCN5A*$^{+/-}$ mouse	23
	Current	+25 %	Canine epicardium	27
		+70 %	Canine midmyocardium	29
		+60 %	Canine midmyocardium	30
		+60 %	Midmyocard. CAVB dogs	30
		+55 %	WT mouse	28
		+40 %	WT and *SCN5A*$^{+/-}$ mouse	23
J_{SERCA}	mRNA (*SERCA2a*)	↔	Control rat myocardium	33
		↔	WT mouse	28
	mRNA (*PLN*)	↔	Control rat myocardium	33
		↔	WT mouse	28
	Protein (SERCA2a)	-14 %	Control rat myocardium	26
	Protein (PLB)	-17 %	Control rat myocardium	26
	Activity	-80 %	Control rat myocardium	38
		-75 %	Control rat myocardium	26
		-35 %	Rat 4/8w following MI	38
		-27 %	Canine myocardium	44
		↔	Canine HF model	44
J_{RyR}	mRNA (*RyR2*)	+22 %	Human myopathic hearts	34
		-32 %	Canine myocardium	41
		↔	Canine ARVC model	41
		↔	WT mouse	28
	Protein (RyR2)	-55 %	Canine myocardium	41
		↔	Canine ARVC model	41

 # = nonsignificant difference. CAVB = complete atrioventricular block; LV = left ventricle; RV = right ventricle; WT= wild-type. See text and Figure 2 for abbreviation of ion currents. Orange = genes (mRNA); Green = protein; Blue = function (current or activity).

of the LV, arising from the first heart field, and the RV, arising from the second heart field.[5,51] Furthermore, within the RV there are embryological differences between the RV free wall and the outflow tract, with the latter forming at a later stage during development.[52] Each developmental origin is associated with expression of different transcription factors.[5] For example, Hand1 is predominantly found in the first heart field, and Hand2 in the second heart field. Similarly Tbx2 is specifically found in the outflow tract of the embryonic heart.[52] Although the exact factors regulating mRNA expression of each ion channel remain largely unknown, the distinct expression profiles of ion channels and Ca^{2+} handling proteins in the LV and RV (see *Table 1*) strongly suggest a role for chamber-specific transcriptional regulation. Quantitative differences between mRNA, protein and current levels in LV versus RV suggest other potential forms of regulation, which may include transcriptional regulation of regulatory subunits or other components of the macromolecular ion-channel complex; microRNA-dependent regulation of protein levels; differences in trafficking, membrane insertion or degradation; distinct subcellular localisation or post-translational modification.[53,1,45,54]

Clinical implications

Due to its unique geometry and cell biology the RV behaves differently from the LV in a variety of pathophysiological conditions and deterioration of right ventricular function strongly predicts clinical outcomes in a variety of circumstances.[13,55] In addition to these structural aspects, Brugada syndrome (BrS) provides an example of the relevance of interventricular electrophysiological differences for arrhythmogenesis. BrS is characterised by right-precordial ST-segment elevation on the body-surface electrocardiogram (ECG) and is associated with an increased risk for sudden cardiac death due to malignant ventricular tachyarrhythmias.[56,57] It was traditionally considered a congenital channelopathy in the absence of overt structural heart disease, linked predominantly to loss-of-function mutations in the *SCN5A* gene (locus 3p21) encoding the pore-forming α subunit of the Na^+ channel. However, recent work has demonstrated the greater complexity of the disease, with at least 18 other genes as well as acquired functional and structural abnormalities also implicated.[58,57]

Two arrhythmogenic mechanisms have generally been proposed for BrS.[57,59] In the repolarisation disorder hypothesis, the loss of I_{Na} in combination with a large I_{to} in the RV epicardium, particularly near the RV outflow tract, results in a local loss of AP spike-and-dome morphology and pronounced regional APD shortening, producing ST-segment elevation in the right-precordial leads. The resulting repolarisation gradient could predispose to ventricular arrhythmogenesis via phase-2 reentry.[60] The depolarisation hypothesis, on the other hand, is based on delayed activation of the RV outflow tract, resulting in large potential gradients that produce the ST-segment elevation.

Recent work in post-mortem hearts with familial BrS indeed found evidence for increased local levels of fibrosis and reduced levels of gap-junction proteins (notably connexin-43) in the RV outflow tract,[61] supporting a role for region-specific structural abnormalities and conduction disturbances in BrS. A mouse model with heterozygous knock-out of *SCN5A* has also suggested that the RV might be particularly sensitive to loss of functional Na^+ channels, with a larger reduction in I_{Na} in RV compared with LV.[23] Similarly, Veeraraghavan and Poelzing[35] showed that heterogeneity in $Na_v1.5$ expression in guinea pig may become a significant determinant of conduction heterogeneities under conditions where I_{Na} is functionally reduced. However, this study also highlights that conduction heterogeneities can be further modulated by interventricular differences in other ion channels, including I_{K1}.[35] Indeed, recent non-invasive eletrocardiographic imaging of BrS patients revealed both slow, discontinuous conduction and steep repolarisation gradients in the RV outflow tract, suggesting interactions between both mechanisms.[14] Thus, regardless of the exact mechanism (depolarisation versus repolarisation), RV-specific electrophysiological and structural properties play a critical role in the phenotypic presentation of BrS patients.

Besides BrS, interventricular electrophysiological differences may play a role in ventricular arrhythmogenesis in a variety of conditions. In general, steep repolarisation gradients have been considered proarrhythmic, and interventricular differences in ion-channel expression, regulation or disease-related remodeling may contribute to such gradients.[5] For example, interventricular differences in I_{KATP} could be an important determinant of LV/RV APD gradients during global ischaemia,[32] and heterogeneous ventricular chamber responses to hypokalaemia and I_{K1} blockade contributed to bifurcated T-wave patterns in guinea pig.[62] Similarly, differential downregulation of RV and LV delayed rectifier K^+ currents could contribute to repolarisation abnormalities and arrhythmogenesis in patients with cardiac hypertrophy or failure.[30]

Conclusion

Chamber-specific heterogeneity in cardiac electrophysiology is a physiological phenomenon, which contributes to fine-tuning of cardiac function. During the last two decades some studies have started to identify differences in ion channel expression and function between RV and LV. However, only limited information is available about the distinct remodeling of each ventricle and the subsequent impact on cardiac arrhythmogenesis. This holds particularly true for post-translational modifications affecting channel function and cardiomyocyte Ca^{2+} handling. Further extensive work, ideally in human samples or large animal models, is needed to define the precise role of interventricular electrophysiological differences in ventricular remodeling, cardiac dysfunction and arrhythmogenesis. ■

1. Bartos DC, Grandi E, Ripplinger CM. Ion channels in the heart. *Compr Physiol* 2015;**5**:1423–64. DOI: 10.1002/cphy.c140069; PMID: 26140724; PMCID: PMC4516287
2. Schram G, Pourrier M, Melnyk P, et al. Differential distribution of cardiac ion channel expression as a basis for regional specialization in electrical function. *Circ Res* 2002;**90**:939–50. PMID: 12016259
3. Bootman MD, Higazi DR, Coombes S, et al. Calcium signalling during excitation-contraction coupling in mammalian atrial myocytes. *J Cell Sci* 2006;**119**:3915–25. PMID: 16988026
4. Dobrev D, Teos LY, Lederer WJ. Unique atrial myocyte Ca^{2+} signaling. *J Mol Cell Cardiol* 2009;**46**:448–51. DOI: 10.1016/j.yjmcc.2008.12.004; PMID: 19150353; PMCID: PMC2836229
5. Boukens BJ, Christoffels VM, Coronel R, et al. Developmental basis for electrophysiological heterogeneity in the ventricular and outflow tract myocardium as a substrate for life-threatening ventricular arrhythmias. *Circ Res* 2009;**104**:19–31. DOI: 10.1161/CIRCRESAHA.108.188698; PMID: 19118284
6. Nerbonne JM. Molecular basis of functional voltage-gated K^+ channel diversity in the mammalian myocardium. *J Physiol* 2000;**525** Pt 2:285–98. PMID: 10835033; PMCID: PMC2269952
7. Sicouri S, Antzelevitch C. A subpopulation of cells with unique electrophysiological properties in the deep subepicardium of the canine ventricle. The M cell. *Circ Res* 1991;**68**:1729–41. PMID: 2036721
8. Haissaguerre M, Jais P, Shah DC, et al. Right and left atrial radiofrequency catheter therapy of paroxysmal atrial fibrillation. *J Cardiovasc Electrophysiol* 1996;**7**:1132–44. PMID: 8985802
9. Lazar S, Dixit S, Marchlinski FE, et al. Presence of left-to-right atrial frequency gradient in paroxysmal but not persistent atrial fibrillation in humans. *Circulation* 2004;**110**:3181–6. PMID: 15533867
10. Voigt N, Trausch A, Knaut M, et al. Left-to-right atrial inward rectifier potassium current gradients in patients with paroxysmal versus chronic atrial fibrillation. *Circ Arrhythm Electrophysiol* 2010;**3**:472–80. DOI: 10.1161/CIRCEP.110.954636; PMID: 20657029
11. Ellinghaus P, Scheubel RJ, Dobrev D, et al. Comparing the global MRNA expression profile of human atrial and ventricular myocardium with high-density oligonucleotide arrays. *J Thorac Cardiovasc Surg* 2005;**129**:1383–90. PMID: 15942582
12. Rodriguez B, Li L, Eason JC, et al. Differences between left and right ventricular chamber geometry affect cardiac vulnerability to electric shocks. *Circ Res* 2005;**97**:168–75. PMID: 15976315; PMCID: PMC2925187
13. Walker LA, Buttrick PM. The right ventricle: Biologic insights and response to disease: Updated. *Curr Cardiol Rev* 2013;**9**:73–81. PMID: 23092273; PMCID: PMC3584309

14. Zhang J, Sacher F, Hoffmayer K, et al. Cardiac electrophysiological substrate underlying the ECG phenotype and electrogram abnormalities in Brugada syndrome patients. *Circulation* 2015;**131**:1950–9. DOI: 10.1161/CIRCULATIONAHA.114.013698; PMID: 25810336; PMCID: PMC4452400
15. Bers DM. Calcium cycling and signaling in cardiac myocytes. *Annu Rev Physiol* 2008;**70**:23–49. PMID: 17988210
16. Qu Z, Weiss JN. Mechanisms of ventricular arrhythmias: From molecular fluctuations to electrical turbulence. *Annu Rev Physiol* 2015;**77**:29–55. DOI: 10.1146/annurev-physiol-021014-071622; PMID: 25340965; PMCID: PMC4342983
17. Michael G, Xiao L, Qi XY, et al. Remodelling of cardiac repolarization: How homeostatic responses can lead to arrhythmogenesis. *Cardiovasc Res* 2009;**81**:491–9. DOI: 10.1093/cvr/cvn266; PMID: 18826964
18. Heijman J, Voigt N, Nattel S, et al. Cellular and molecular electrophysiology of atrial fibrillation initiation, maintenance, and progression. *Circ Res* 2014;**114**:1483–99. DOI: 10.1161/CIRCRESAHA.114.302226; PMID: 24763466
19. Llach A, Molina CE, Fernandes J, et al. Sarcoplasmic reticulum and l-type Ca^{2+} channel activity regulate the beat-to-beat stability of calcium handling in human atrial myocytes. *J Physiol* 2011;**589**:3247–62. DOI: 10.1113/jphysiol.2010.197715; PMID: 21521767; PMCID: PMC3145937
20. Molina CE, Llach A, Herraiz-Martinez A, et al. Prevention of adenosine A2A receptor activation diminishes beat-to-beat alternation in human atrial myocytes. *Basic Res Cardiol* 2016;**111**:5. DOI: 10.1007/s00395-015-0525-2; PMID: 26611209
21. Comtois P, Kneller J, Nattel S. Of circles and spirals: Bridging the gap between the leading circle and spiral wave concepts of cardiac reentry. *Europace* 2005;**7** Suppl 2:10–20. PMID: 16102499
22. Pandit SV, Jalife J. Rotors and the dynamics of cardiac fibrillation. *Circ Res* 2013;**112**:849–62. DOI: 10.1161/CIRCRESAHA.111.300158; PMID: 23449547; PMCID: PMC3650644
23. Martin CA, Siedlecka U, Kemmerich K, et al. Reduced Na^+ and higher K^+ channel expression and function contribute to right ventricular origin of arrhythmias in SCN5A +/- mice. *Open Biol* 2012;**2**:120072. DOI: 10.1098/rsob.120072; PMID: 22773948; PMCID: PMC3390792
24. Ramakers C, Stengl M, Spatjens RL, et al. Molecular and electrical characterization of the canine cardiac ventricular septum. *J Mol Cell Cardiol* 2005;**38**:153–61. PMID: 15623432
25. Ramakers C, Vos MA, Doevendans PA, et al. Coordinated down-regulation of KCNQ1 and KCNE1 expression contributes to reduction of I_{Ks} in canine hypertrophied hearts. *Cardiovasc Res* 2003;**57**:486–96. PMID: 12566121
26. Sathish V, Xu A, Karmazyn M, et al. Mechanistic basis of differences in Ca^{2+}-handling properties of sarcoplasmic reticulum in right and left ventricles of normal rat myocardium. *Am J Physiol Heart Circ Physiol* 2006;**291**:H88–96. PMID: 16461368
27. Di Diego JM, Sun ZQ, Antzelevitch C. I_{to} and action potential notch are smaller in left vs. right canine ventricular epicardium. *Am J Physiol* 1996;**271**:H548–61. PMID: 8770096
28. Kondo RP, Dederko DA, Teutsch C, et al. Comparison of contraction and calcium handling between right and left ventricular myocytes from adult mouse heart: A role for repolarization waveform. *J Physiol* 2006;**571**:131–46. PMID: 16357014; PMCID: PMC1805641
29. Volders PG, Sipido KR, Carmeliet E, et al. Repolarizing K^+ currents I_{to1} and I_{Ks} are larger in right than left canine ventricular midmyocardium. *Circulation* 1999;**99**:206–10. PMID: 9892584
30. Volders PG, Sipido KR, Vos MA, et al. Downregulation of delayed rectifier K^+ currents in dogs with chronic complete atrioventricular block and acquired torsades de pointes. *Circulation* 1999;**100**:2455–61. PMID: 10595960
31. Choi SW, Ahn JS, Kim HK, et al. Increased expression of atp-sensitive k channels improves the right ventricular tolerance to hypoxia in rabbit hearts. *Korean J Physiol Pharmacol* 2011;**15**:189–94. DOI: 10.4196/kjpp.2011.15.4.189; PMID: 21994476; PMCID: PMC3186919
32. Pandit SV, Kaur K, Zlochiver S, et al. Left-to-right ventricular differences in I_{KATP} underlie epicardial repolarization gradient during global ischemia. *Heart Rhythm* 2011;**8**:1732–9. DOI: 10.1016/j.hrthm.2011.06.028; PMID: 21723845; PMCID: PMC3244837
33. Correia Pinto J, Henriques-Coelho T, Roncon-Albuquerque R, Jr., et al. Differential right and left ventricular diastolic tolerance to acute afterload and NCX gene expression in Wistar rats. *Physiol Res* 2006;**55**:513–26. PMID: 16343035
34. Sivagangabalan G, Nazzari H, Bignolais O, et al. Regional ion channel gene expression heterogeneity and ventricular fibrillation dynamics in human hearts. *PLoS One* 2014;**9**:e82179. DOI: 10.1371/journal.pone.0082179; PMID: 24427266; PMCID: PMC3888386
35. Veeraraghavan R, Poelzing S. Mechanisms underlying increased right ventricular conduction sensitivity to flecainide challenge. *Cardiovasc Res* 2008;**77**:749–56. PMID: 18056761
36. Samie FH, Berenfeld O, Anumonwo J, et al. Rectification of the background potassium current: A determinant of rotor dynamics in ventricular fibrillation. *Circ Res* 2001;**89**:1216–23. PMID: 11739288
37. Warren M, Guha PK, Berenfeld O, et al. Blockade of the inward rectifying potassium current terminates ventricular fibrillation in the guinea pig heart. *J Cardiovasc Electrophysiol* 2003;**14**:621–31. PMID: 12875424
38. Afzal N, Dhalla NS. Differential changes in left and right ventricular sr calcium transport in congestive heart failure. *Am J Physiol* 1992;**262**:H868–74. PMID: 1313649
39. Luss I, Boknik P, Jones LR, et al. Expression of cardiac calcium regulatory proteins in atrium v ventricle in different species. *J Mol Cell Cardiol* 1999;**31**:1299–314. PMID: 10371704
40. O'Rourke B. The ins and outs of calcium in heart failure. *Circ Res* 2008;102:1301–3. DOI: 10.1161/CIRCRESAHA.108.178095; PMID: 18535266; PMCID: PMC2713010
41. Meurs KM, Lacombe VA, Dryburgh K, et al. Differential expression of the cardiac ryanodine receptor in normal and arrhythmogenic right ventricular cardiomyopathy canine hearts. *Hum Genet* 2006;120:111–8. PMID: 16733711
42. Molina CE, Johnson DM, Mehel H, et al. Interventricular differences in beta-adrenergic responses in the canine heart: Role of phosphodiesterases. *J Am Heart Assoc* 2014;3:e000858. DOI: 10.1161/JAHA.114.000858; PMID: 24904016; PMCID: PMC4309082
43. Kleiman RB, Houser SR. Electrophysiologic and mechanical properties of single feline RV and LV myocytes. *J Mol Cell Cardiol* 1988;20:973–82. PMID: 3236385
44. Gupta RC, Shimoyama H, Tanimura M, et al. Sr Ca^{2+}-ATPase activity and expression in ventricular myocardium of dogs with heart failure. *Am J Physiol* 1997;**273**:H12–8. PMID: 9249469
45. Heijman J, Dewenter M, El-Armouche A, et al. Function and regulation of serine/threonine phosphatases in the healthy and diseased heart. *J Mol Cell Cardiol* 2013;**64**:90–8. DOI: 10.1016/j.yjmcc.2013.09.006; PMID: 24051368
46. Lymperopoulos A, Rengo G, Koch WJ. Adrenergic nervous system in heart failure: Pathophysiology and therapy. *Circ Res* 2013;**113**:739–53. DOI: 10.1161/CIRCRESAHA.113.300308; PMID: 23989716; PMCID: PMC3843360
47. Rapundalo ST. Cardiac protein phosphorylation: functional and pathophysiological correlates. *Cardiovasc Res* 1998;**38**:559–88. PMID: 9747427
48. Wang GY, McCloskey DT, Turcato S, et al. Contrasting inotropic responses to α_1-adrenergic receptor stimulation in left versus right ventricular myocardium. *Am J Physiol Heart Circ Physiol* 2006;**291**:H2013–7. PMID: 16731650
49. Chu C, Thai K, Park KW, et al. Intraventricular and interventricular cellular heterogeneity of inotropic responses to α_1-adrenergic stimulation. *Am J Physiol Heart Circ Physiol* 2013;**304**:H946–53. DOI: 10.1152/ajpheart.00822.2012; PMID: 23355341; PMCID: PMC3625891
50. Spasojevic N, Gavrilovic L, Dronjak S. Regulation of catecholamine-synthesising enzymes and beta-adrenoceptors gene expression in ventricles of stressed rats. *Physiol Res* 2011;**60** Suppl 1:S171–6. PMID: 21777029
51. Buckingham M, Meilhac S, Zaffran S. Building the mammalian heart from two sources of myocardial cells. *Nat Rev Genet* 2005;**6**:826–35. PMID: 16304598
52. Boukens BJ, Coronel R, Christoffels VM. Embryonic development of the right ventricular outflow tract and arrhythmias. *Heart Rhythm* 2016;**13**:616–22. DOI: 10.1016/j.hrthm.2015.11.014; PMID: 26586454
53. Balijepalli RC, Kamp TJ. Caveolae, ion channels and cardiac arrhythmias. *Prog Biophys Mol Biol* 2008;**98**:149–60. DOI: 10.1016/j.pbiomolbio.2009.01.012; PMID: 19351512; PMCID: PMC2836876
54. Meadows LS, Isom LL. Sodium channels as macromolecular complexes: Implications for inherited arrhythmia syndromes. *Cardiovasc Res* 2005;**67**:448–58. PMID: 15919069
55. Leite-Moreira AF, Lourenco AP, Balligand JL, et al. ESC working group on myocardial function position paper: How to study the right ventricle in experimental models. *Eur J Heart Fail* 2014;**16**:509–18. DOI: 10.1002/ejhf.66; PMID: 24574252
56. Brugada P, Brugada J. Right bundle branch block, persistent ST segment elevation and sudden cardiac death: A distinct clinical and electrocardiographic syndrome. A multicenter report. *J Am Coll Cardiol* 1992;**20**:1391–6. PMID: 1309182
57. Hoogendijk MG, Opthof T, Postema PG, et al. The Brugada ECG pattern: A marker of channelopathy, structural heart disease, or neither? Toward a unifying mechanism of the brugada syndrome. *Circ Arrhythm Electrophysiol* 2010;**3**:283–90. DOI: 10.1161/CIRCEP.110.937029; PMID: 20551422
58. Antzelevitch C, Patocskai B. Brugada syndrome: Clinical, genetic, molecular, cellular, and ionic aspects. *Curr Probl Cardiol* 2016;**41**:7–57. DOI: 10.1016/j.cpcardiol.2015.06.002; PMID: 26671757; PMCID: PMC4737702
59. Meregalli PG, Wilde AA, Tan HL. Pathophysiological mechanisms of Brugada syndrome: Depolarization disorder, repolarization disorder, or more? *Cardiovasc Res* 2005;**67**:367–78. PMID: 15913579
60. Antzelevitch C. The Brugada syndrome: Ionic basis and arrhythmia mechanisms. *J Cardiovasc Electrophysiol* 2001;**12**:268–72. PMID: 11232628
61. Nademanee K, Raju H, de Noronha SV, et al. Fibrosis, connexin-43, and conduction abnormalities in the Brugada syndrome. *J Am Coll Cardiol* 2015;**66**:1976–86. DOI: 10.1016/j.jacc.2015.08.862; PMID: 26516000; PMCID: PMC4631798
62. Poelzing S, Veeraraghavan R. Heterogeneous ventricular chamber response to hypokalemia and inward rectifier potassium channel blockade underlies bifurcated t wave in guinea pig. *Am J Physiol Heart Circ Physiol* 2007;**292**:H3043–51. PMID: 17307991
63. Nerbonne JM, Kass RS. Molecular physiology of cardiac repolarization. *Physiol Rev* 2005;**85**:1205–53. PMID: 16183911
64. Volders PG, Sipido KR, Vos MA, et al. Cellular basis of biventricular hypertrophy and arrhythmogenesis in dogs with chronic complete atrioventricular block and acquired torsade de pointes. *Circulation* 1998;**98**:1136–47. PMID: 9736601
65. Teutsch C, Kondo RP, Dederko DA, et al. Spatial distributions of Kv4 channels and KChip2 isoforms in the murine heart based on laser capture microdissection. *Cardiovasc Res* 2007;**73**:739–49. PMID: 17289005
66. Luo X, Xiao J, Lin H, et al. Genomic structure, transcriptional control, and tissue distribution of HERG1 and KCNQ1 genes. *Am J Physiol Heart Circ Physiol* 2008;**294**:H1371–80. DOI: 10.1152/ajpheart.01026.2007; PMID: 18192214